Bull. Mater. Sci., Vol. 39, No. 4, August 2016, pp. 953–960. © Indian Academy of Sciences.
DOI 10.1007/s12034-016-1183-1

Synthesis and investigation of silicon carbide nanowires by HFCVD method

S H MORTAZAVI*, M GHORANNEVISS, M DADASHBABA and R ALIPOUR
Plasma Physics Research Center, Science and Research Branch, Islamic Azad University, Tehran, Iran

MS received 16 September 2015; accepted 17 November 2015

Abstract. **Silicon carbide (SiC) nanowire has been fabricated by hot filament chemical vapour deposition (HFCVD) mechanism in the temperature range of 600–800°C. Synthesis is performed under vacuum in the atmospheres of hexamethyldisiloxane/alcohol (HMDSO/C_2H_5OH) vapour and hydrogen (H_2) gas mixture. In this research dependence of SiC properties on temperature is discussed. Morphology and structural properties of SiC nanowire grown on glass substrate were characterized by field emission scanning electron microscopy (FESEM), X-ray diffraction (XRD), energy diffraction spectrometer (EDX), and four-point probe (4PP). Also Mountains Map Premium (64-bit version) software is used to investigate morphological features of samples. In this context, the analysis of the motifs, depth histograms, statistical parameters, texture direction, fractal, and the peak count histograms of the nanostructure surface of samples are carried out. According to analysis, SiC films had a good crystal quality without defects or low residual stress. We found that increasing substrate temperature increases silicon and oxygen doping amount. We also found that electrical resistivity and surface roughness increased by increasing substrate temperature. This study showed that SiC nanowires with high density grew on the free catalyst glass substrate, and the alignment of SiC nanowires decreased.**

Keywords. **Silicon carbide; nanowires; HFCVD method; surface properties.**

1. Introduction

SiC is a wide band gap material with well-recognized potential for high (power, temperature, frequency, thermal conductivity, break down field, and saturation velocity). Compared to other wide band gap semiconductors, the availability of SiC substrates for homoepitaxy is a big advantage. The basic parameters of SiC material are attractive for semiconductor devices fabrication with superior characteristics for industrial needs in aircraft, space electronics, automotive, and power utility industries. Silicon carbide materials, especially one-dimensional SiC, such as nanowires and nanorods, are of great interest for many applications because of their mentioned excellent properties. For example, SiC nanowire is widely considered as a reinforcement material [1–4]. SiC has many applications because it is possible to prepare various forms such as fibre, matrix, and composite from organic liquid or vapour precursors.

So it is possible to adjust the crystallinity from amorphous to crystalline state including intermediate nanocrystalline state. Recently one-dimensional (1D) semiconductor nanostructures (wires, rods, belts and tubes) have become the focus of intensive research because of their unique application in electronic, optoelectronic, and sensor devices on a nanometre scale. They possess novel properties intrinsically associated with low dimensionality and size confinement, which make 'bottom-up' construction of nanodevices possible [5–11]. Because of their potential applications in nanodevices, 1D semiconductor nanomaterials were selected as one of the top 10 technologies by the MIT Technical review in 2003 [12]. Among these semiconductor nanowires, SiC has very unique properties, such as wide band gap, excellent thermal conductivity, chemical inertness, high electron mobility and biocompatibility, which promise well for applications in microelectronics and optoelectronics, therefore it has attracted much interest from the materials and devices communities [13–15].

In 1995 Dai *et al* [16] reported the first SiC nanowire synthesis by the reaction of carbon nanotubes with either silicon monoxide or silicon and iodine vapour. The uniqueness of silicon carbide properties arise from the nature of the bond. Si–C bond as Si–O and Si–N bonds is among the strongest chemical bonds in the matter. Thus, this provides a good chemical and thermal stability as well as very high melting temperature, high mechanical properties, and hardness [17]. Some of these properties are directly linked to the SiC structure that alternates the Si and C atom layers, for example value of the thermal conductivity can be varied with doping. As it is known, silicon carbide crystallizes in many polytypes of polymorphs in one measurement, and its total amount is more than 200 [18]. The SiC polytype content is defined by conditions of preparation such as temperature, pressure, environment, and impurities [19]. Synthesis of SiC nanowires can be carried out by various methods such as HFCVD [20–23], APCVD [24],

*Author for correspondence (hamideh.mortazavi@srbiau.ac.ir)

ECR–CVD [25], PECVD [26], and so on. HFCVD is an effective method for growing diamond films. This method has been used for synthesizing films and nanorods since several years ago.

This research was conducted to manufacture SiC nanowires by hot filament chemical vapour deposition (HFCVD) method on glass samples at various substrate temperatures in the same contents of HMDSO/H_2 mixed gas flux. Also we need to mention that we have not used any metal catalyst in this work because it is difficult to remove the catalyst after the synthesis process and the metal catalyst remains in the SiC nanowires functions as an impurity, and can cause changes in the mechanical properties of thin films [27–29]. Moreover, the effects of substrate temperature on physical transformations of the SiC nanowires are presented.

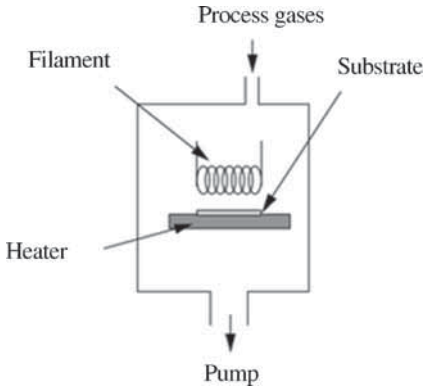

Figure 1. Schematic of hot filament chemical vapour deposition setup.

2. Experimental

In this experiment, synthesis of silicon carbide (SiC) nanowire was carried out by HFCVD system. HFCVD system was composed of a stainless steel chamber, gas inlet, vacuum pump, heater, tungsten filament, and HMDSO evaporation container (figure 1). Tungsten filament was constantly heated to 2000°C during the experiment and the temperature of the substrates was fixed at 600, 700, and 800°C. The glass used as substrate was cleaned by using acetone, alcohol, and deionized (DI) water. The distance between filament and glass substrate was 1 cm. The chamber was first pumped to 1×10^{-5} Torr by mechanical and diffusion vacuum pumps, then high purity H_2 gas was fed into it. Also a mixture of HMDSO/C_2H_5OH vapor was used as hydrocarbon and silicon source [30–35].

3. Result and discussion

Synthesized SiC nanowires were investigated by different methods, and the structure of SiC thin films was characterized

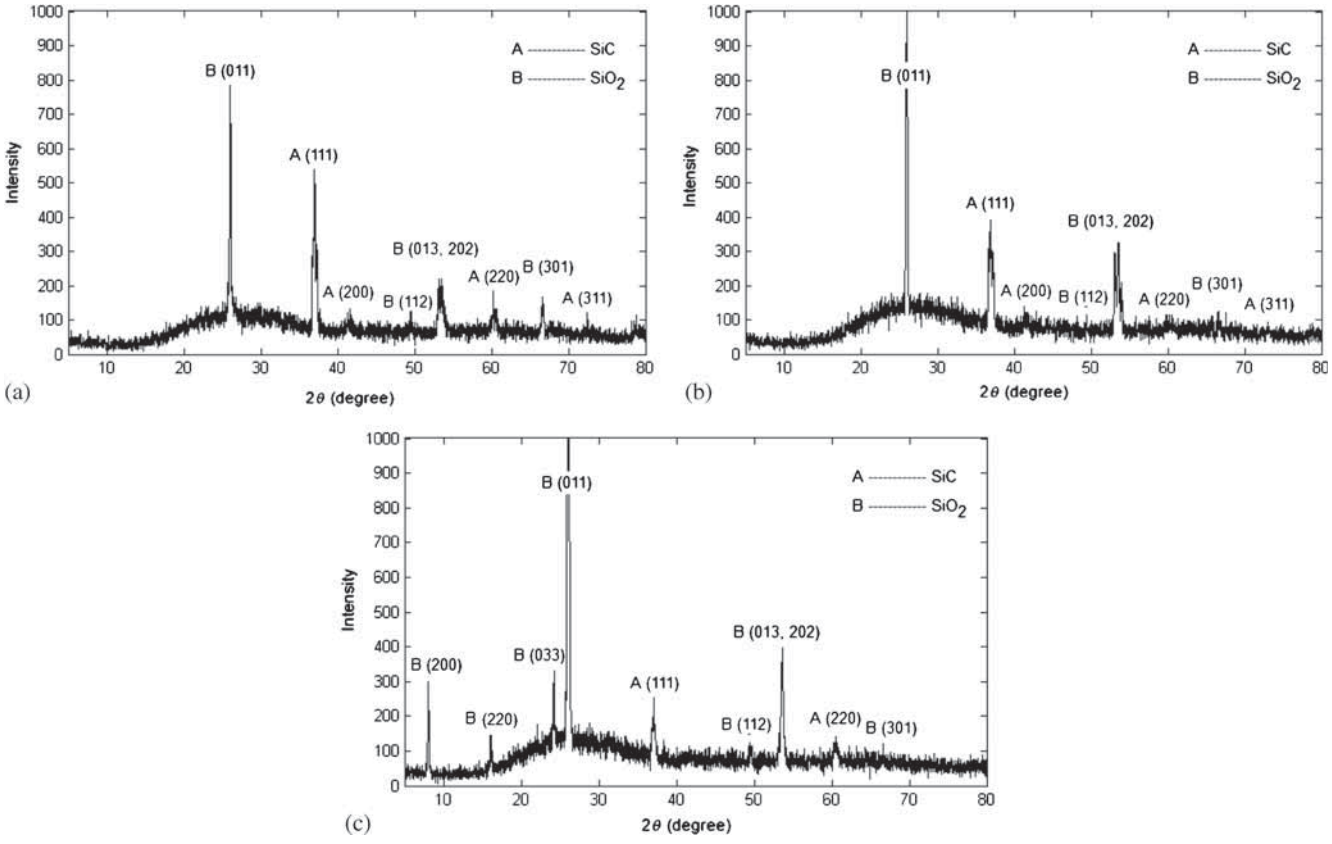

Figure 2. XRD spectrum of silicon carbide nanowire at different substrate temperatures of (**a**) 600, (**b**) 700 and (**c**) 800°C.

by X-ray diffraction (XRD). The XRD equipment was a Philips X-pert system using CuKα radiation (wavelength = 1.5405 Å with a tungsten filament at 40 kV and 40 mA). According to standard PDF card numbers of 01-080-2146 and 00-044-0696, silicon dioxide (SiO_2), and according to standard PDF card numbers of 01-074-2307 and 01-073-1663, SiC structures had grown on the surface. Figure 2 shows XRD results for SiC films which are grown at different substrate temperatures of 600, 700, and 800°C.

XRD spectra shows both structures of hexagonal, and cubic SiC, (111, 200, 220 and 311), and both structures of hexagonal and orthorhombic SiO_2 (011, 112, 013, 202, 301, 200, 220 and 033) which were grown on the substrates. As can be seen in figure 2, by increasing substrate temperature, the peaks of SiC have decreased and those of SiO_2 have increased, also the peaks related to SiO_2 orthorhombic structure (200, 220 and 033) with PDF card number of 00-044-0696 appeared at above 700°C, and they are related to low SiC density at high temperature. Also results showed that, with substrate temperature, oxygen and silicon concentration increased and the carbon concentration decreased. This means that more oxygen and silicon are formed from raw materials than carbon. According to figure 2 we found that rising temperature led to rising the peak of SiO_2. Since SiO_2 is one of the high resistance materials, it is expected that by increasing temperature, the sample resistance increases. Improving the quality of silicon carbide crystalline is highly dependent on substrate temperature, such that SiC film grown at higher temperatures (800°C) had the best quality. The SiC film grown on the glass substrate has good single-crystalline quality without grain boundaries.

Figure 3 shows the FESEM images of the nanowires synthesized at different temperatures of 600, 700, and 800°C. According to observation, high dense hexagonal nanowires randomly grew on the substrate. With a rise in temperature, nanowires gradually grew in all dimensions, but growth in the surface normal vector direction was more than that of other directions. Nanowires in vicinity of the larger ones were unable to have dimensional growth and remained so small. This can be due to shadowing phenomenon. Also the lengths of nanowires synthesized at 800°C, were much longer than those synthesized at 600 and 700°C. In brief, the height of nanowires remained too small at lower substrate temperatures. The growth temperature has a great impact on the synthesis of SiC, such that by increasing the temperature it is possible to use a wider range of parameters and to reach higher growth rates as a result [35–38].

The results in table 1 shows motifs detection of specifications on surfaces and analysis according to ISO 25178

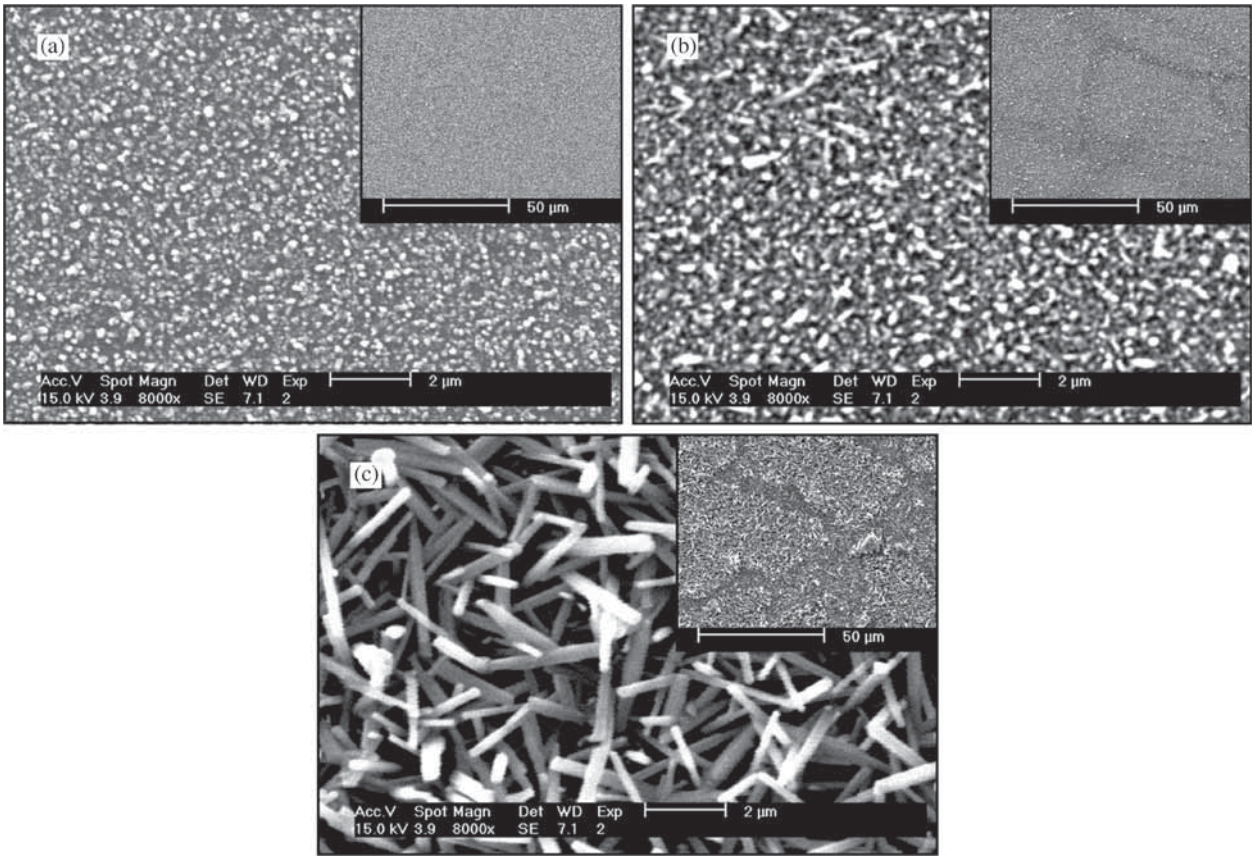

Figure 3. FESEM image of synthesized SiC nanowires on the glass substrates at different temperatures of (**a**) 600, (**b**) 700 and (**c**) 800°C.

Table 1. Motifs analysis according to ISO 25178 for samples of SiC thin films at different substrate temperatures of 600, 700 and 800°C.

Parameters	Sample a	Sample b	Sample c
Number of motifs	1170	689	158
Mean area (μm^2)	0.05500517041	0.09340500636	0.4073167682
Mean of Nb of neighbours	5.721367521	5.651669086	5.253164557
Mean of mean diameter (μm)	0.2264269284	0.296698382	0.5862017503
Mean of equivalent diameter (μm)	0.2310434272	0.3030804556	0.6236945555
Mean form factor	0.6454293711	0.6455254906	0.5158920613
Mean roundness	0.5431011405	0.5554913804	0.5048571372
Mean orientation (°)	96.47725938	85.66826715	90.12813317

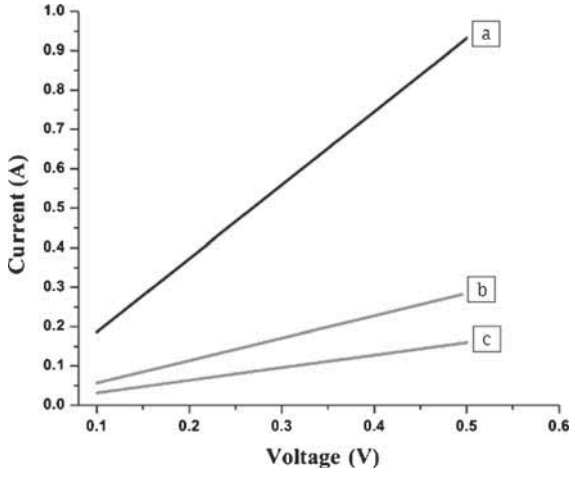

Figure 4. Current–voltage characteristics of SiC surface at different substrate temperatures of (a) 600, (b) 700 and (c) 800°C.

[39] detection algorithms (segmentation by watersheds). The watershed segmentation is a mathematical morphological tool for image segmentation based on geodesic operators which can automatically segment images into a series of closed segmentation regions [40]. Mountains Map Premium software was used to calculate motifs analysis in this research [41].

We also carried out an I–V measurement using the standard four-probe method. I–V measurements are mainly used to determine conductivity of the SiC film. According to I–V data, the resistivity of SiC films is ohmic and had a rising trend with temperature, as expected from XRD results in figure 2. I–V characteristic curves of SiC films are shown in figure 4. This figure shows increasing temperature, decreases the slop of I–V graph.

EDX results also showed that by increasing temperature, the amount of silicon and oxygen doped increased, although that of carbon doped decreased. Besides, this resistivity increase may be due to increased oxygen and decreased carbon (table 2). On the one hand, the high electronegativity of oxygen can lead to accumulation of charge carriers, on the other hand, because of high electronegativity of oxygen, the charge carriers are bound to the network and then this charge carrier's deficiency can increase the resistance of the film. Also carbon that is a factor in conductivity, decreased with rising temperature and this may lead to an increase in resistivity. EDX, four point probe, XRD, and I–V graph are all in agreement and they confirm our previous explanation.

By increasing the substrate temperature, the length of the nanowires were increased, while their cross-section was decreased. In this work, various factors such as rising the length, decreasing cross-sectional area of nanowires, increasing

Table 2. EDX and four-point probe (4PP).

Samples	Substrate temperature (°C)	O_2 (%)	C (%)	Si (%)	4PP (Ω)
a	600	51.44	34.03	14.53	10.80
b	700	57.25	26.84	15.91	12.20
c	800	60.47	21.70	17.83	13.00

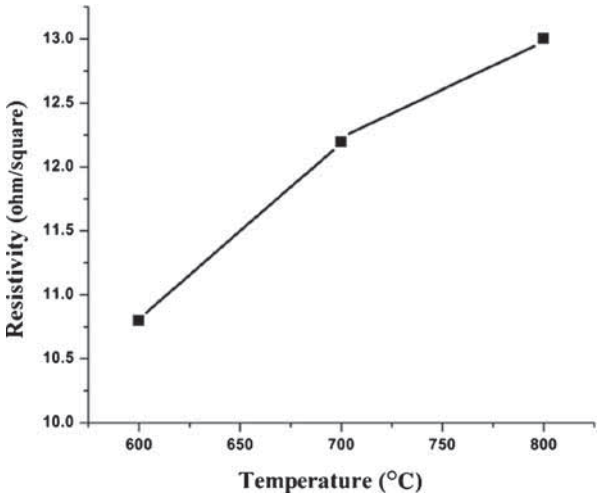

Figure 5. Plot of resistivity of SiC film as a function of substrate temperature.

oxygen doped, and decreasing carbon doped, all affect electrical properties of the film. By considering these, according to equation (1), it can be shown that the resistivity has been increased.

$$R = \rho \frac{L}{A}, \tag{1}$$

where R, A, L, and ρ are resistivity, cross-sectional area, length, and specific resistivity, respectively, the results are shown in figure 5.

Figure 6 shows the depth histograms associated with FESEM images in figure 3. The depth histogram presents the density of the dispensation of the points on the surface. The Abbott–Firestone curve or bearing area curve (BAC) describes the surface texture of an object. The curve could be found from a profile trace by drawing lines parallel to the datum and by measuring the fraction of the line which lies in the profile [42]. Mathematically, it is the cumulative probability density function of the surface profile height and can be calculated by integrating the profile trace [43]. It is useful to understand the properties of sealing and bearing surfaces. The shape of the curve is distilled into several the surface roughness parameters, especially the Rk family of parameters. The Abbott–Firestone curve is overlaid in red. The vertical axis is scaled in depths and the horizontal axis is scaled in percentage of the total population. This curve represents the bearing ratio curve; it means that for a specific depth, the percentage of the material traversed in relation to the area covered. This function is a cumulative function of the amplitude distribution. Material ratio curve (figure 6, red plot) is the integral of the amplitude distribution function (ADF/surface histogram). It is an accumulative probability distribution and a criterion for the material to air ratio, expressed as a percentage at a specific depth below the highest peak on the surface. At the highest peak, ratio of the material to air is 0%, where this ratio at the deepest valley is 100%. The horizontal axis shows the bearing ratio (%), while the vertical axis shows the depth measurement unit.

Some of the statistical parameters of the surface of SiC thin films at different substrate temperatures; at (a) 600, (b) 700, and (c) 800°C, according to ISO 25178 [39] are presented in table 3. As one of the results of table 3, it can be noted that the kurtosis limit is more than 3 for sample a. Also this limit is less than 3 for samples b and c. The kurtosis is qualifying the flatness of the height distribution. For spiky surfaces sku $>$ 3, for bumpy surfaces sku $<$ 3 and for the random surfaces sku $=$ 3.

Table 4 shows some of the parameters calculated for the most important texture directions specified in the SiC thin film surfaces. The texture direction study analyzes the surface using the Fourier transform and shows dominant surface directions on a polar or Cartesian plot [41].

Fractal analysis of a surface or profile displays a scatter plot using the enclosing box method or the morphological envelope method. It calculates the fractal feature, the slope of the regression line, and the correlation coefficient of the regression line. These results are shown in figure 7 and table 5. The slope of a plot of log (N (L)) compared with log (1/L) gives the fractal dimension when L and N (L) are the lattice constant and the number of all

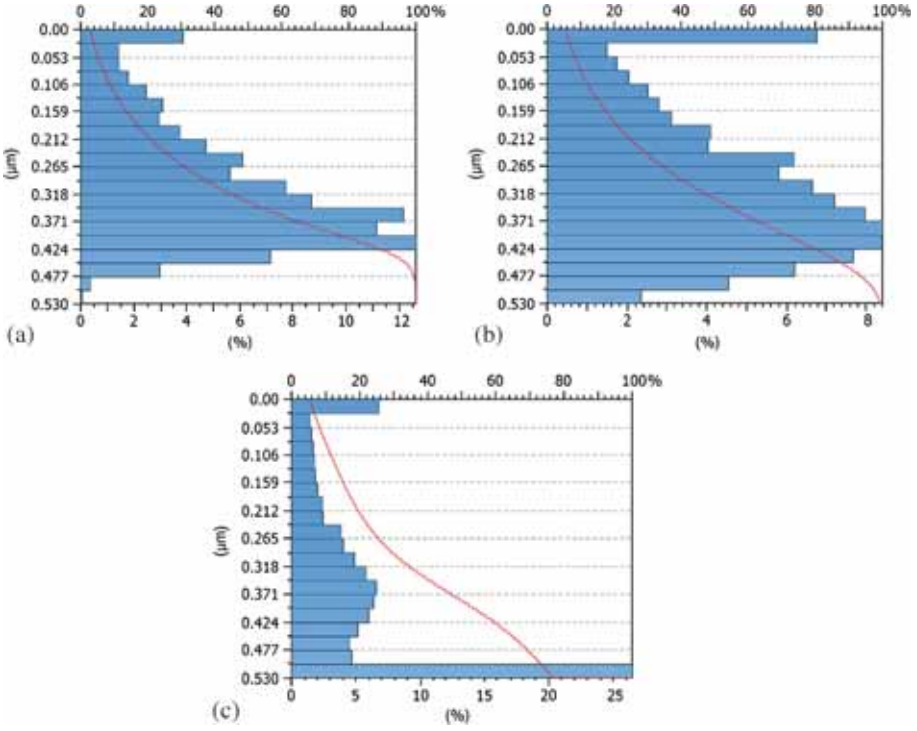

Figure 6. The depth histograms of the nanostructure surfaces of SiC samples at different substrate temperatures of (**a**) 600, (**b**) 700 and (**c**) 800°C.

Table 3. The statistical parameters for samples of SEM images of SiC films according to ISO 25178.

Statistical parameters	Sample a	Sample b	Sample c
Height parameters			
Root mean square height, Sq (μm)	0.1177165365	0.1393476781	0.1625952008
Skewness, Ssk	0.9111797733	0.6312471966	0.7480230097
Kurtosis, Sku	3.070919924	2.532611343	2.539178799
Maximum peak height, Sp (μm)	0.3025387885	0.301358	0.3550046
Maximum pit height, Sv (μm)	0.2274612115	0.228642	0.1749954
Maximum height, Sz (μm)	0.53	0.53	0.53
Arithmetic mean height, Sa (μm)	0.09514215894	0.1142131371	0.1331909592
Functional parameters			
Areal material ratio, Smr (%)	100	100	100
Inverse areal material ratio, Smc (μm)	0.1805581838	0.2186648151	0.2719444406
Extreme peak height, Sxp (μm)	0.1179309347	0.1763737647	0.146009042
Spatial parameters			
Auto-correlation length, Sal (μm)	0.08381768074	0.115046521	0.2989706681
Texture-aspect ratio, Str	0.7907056042	0.7675444265	0.8411261526
Texture direction, Std (°)	160.2507994	3.746364344	166.7459519
Hybrid parameters			
Root mean square gradient, Sdq	4.157635431	2.996175676	2.887876782
Developed interfacial area ratio, Sdr (%)	271.3592772	176.9397981	152.7917299
Functional parameters (volume)			
Material volume, Vm ($\mu m^3\ \mu m^{-2}$)	0.00718494658	0.00629167888	0.006261024398
Void volume, Vv ($\mu m^3\ \mu m^{-2}$)	0.1877440574	0.2249589551	0.2782073495
Peak material volume, Vmp ($\mu m^3\ \mu m^{-2}$)	0.00718494658	0.00629167888	0.006261024398
Core material volume, Vmc ($\mu m^3\ \mu m^{-2}$)	0.09986649415	0.126233213	0.1683965328
Core void volume, Vvc ($\mu m^3\ \mu m^{-2}$)	0.1825979474	0.216909987	0.2781019672
Pit void volume, Vvv ($\mu m^3\ \mu m^{-2}$)	0.005146110008	0.008048968119	0.0001053823221
Feature parameters			
Mean dale area, Sda (μm^2)	0.02445361178	0.08394258163	0.04424346326
Mean hill area, Sha (μm^2)	0.02892471179	0.08135485913	0.03324378315
Mean dale volume, Sdv (μm^3)	9.772978351e-005	0.0007110296841	0.0006492264747
Mean hill volume, Shv (μm^3)	0.0006504536564	0.002125088102	0.000189006565

Table 4. The texture direction for the samples of SiC thin films.

The texture direction (surface)	Isotropy (%)	First direction (°)	Second direction (°)	Third direction (°)
Sample a	79.1	0.165	135	45.0
Sample b	76.8	0.0968	45.0	90.0
Sample c	84.1	26.5	154	45.0

Table 5. Fractal analysis results obtained by the enclosing box method for samples of SiC thin films at different substrate temperatures.

Parameters	Sample a (600°C)	Sample b (700°C)	Sample c (800°C)
Fractal dimension	2.85	2.82	2.66
Slope (1)	−2.85	−2.82	−2.66
R^2 (1)	1.00	0.999	0.998
Slope (2)	−2.85	−2.82	−2.66
R^2 (2)	1.00	0.999	0.998

cubes that contain at least one pixel of the image, respectively [44]. Also, the peak count histograms are shown in figure 8.

4. Conclusion

In summary, SiC nanowires were synthesized by a reaction of HMDSO in H_2 atmosphere at different substrate temperatures of 600, 700, and 800°C without the use of any metal catalyst. XRD spectra showed that both structures of hexagonal and cubic SiC and both structures of hexagonal and orthorhombic SiO_2 were grown on the substrates from one-precursor of HMDSO in H_2 atmosphere. Also we observed that with increasing the substrate temperature over 700°C, the peaks related to SiO_2 orthorhombic structure appeared. SiC film had a good crystal quality without defect. So, we can conclude that rising substrate temperature improves the quality of silicon carbide films by enlarging the crystal sizes. FESEM analysis showed that with rising temperature, grain size of nanowires and subsequently surface roughness significantly increased. It could also be seen that by rising substrate temperature, the SiC grain size and electrical resistivity increased. It was also clear that the SiC grain size and electrical resistivity were increased by rising

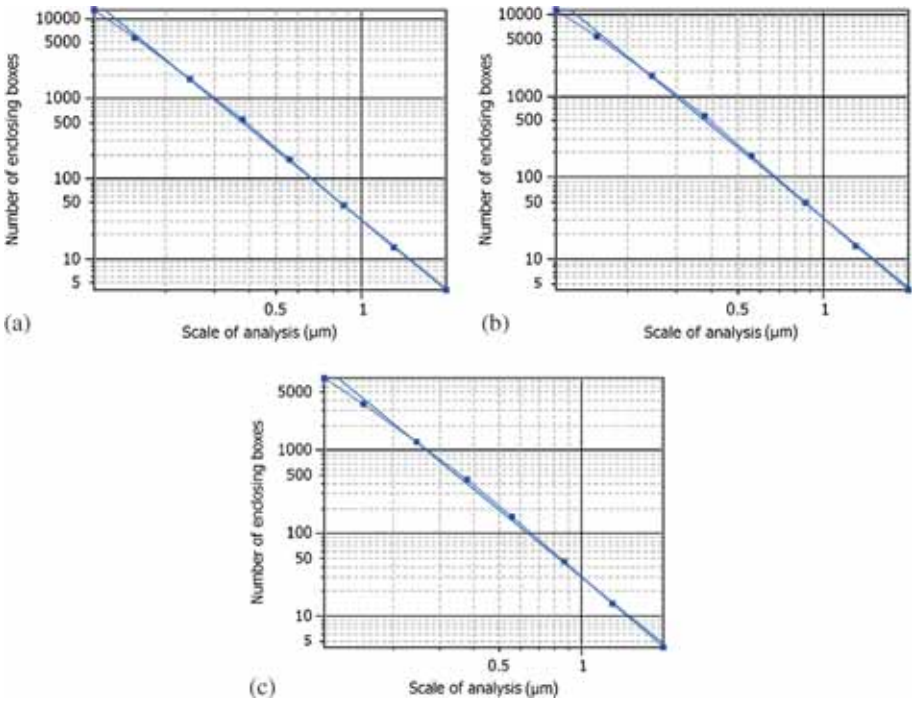

Figure 7. The fractal analysis results obtained by enclosing box method for SiC samples at different substrate temperatures: (**a**) 600, (**b**) 700 and (**c**) 800°C.

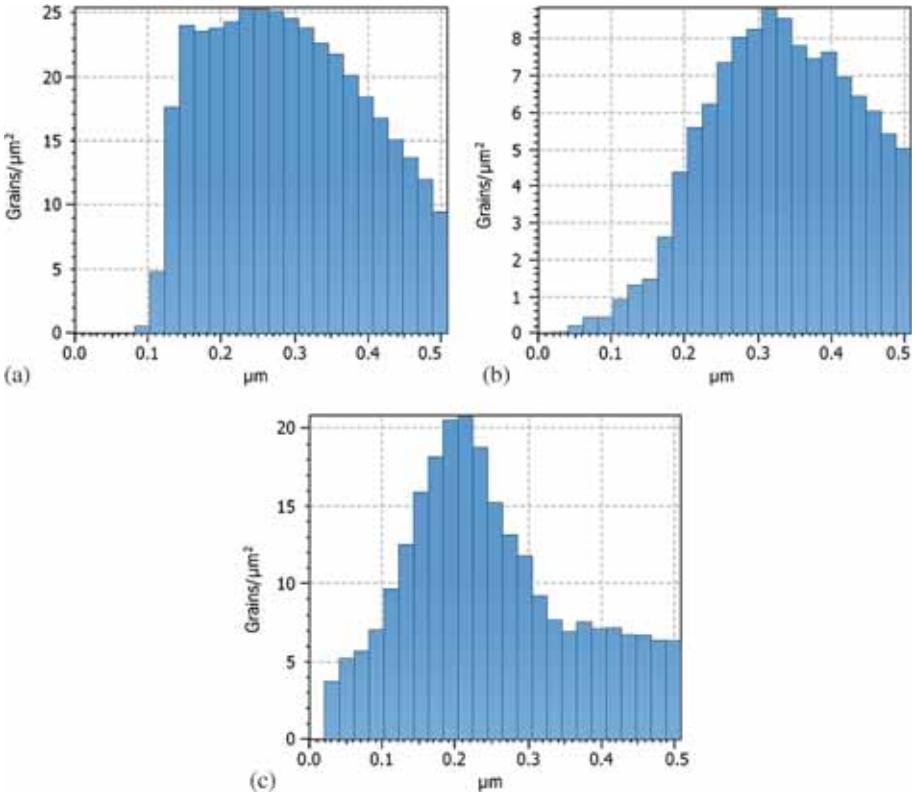

Figure 8. The peak count histograms of the nanostructure surfaces of SiC samples at different substrate temperatures of (**a**) 600, (**b**) 700 and (**c**) 800°C.

substrate temperature. EDX results showed rising temperature, increases oxygen and decreases carbon doped. This rise in electrical resistance could be due to increased oxygen and decreased carbon, but the amount of oxygen doped has dramatic effects than the carbon doped. Also, to investigate the morphological features of samples, the Mountains Map Premium (64-bit version) software was used. In this context, analysis of motifs, depth histograms, statistical parameters, texture direction, fractal, and peak count histograms of the nanostructure surface of samples were carried out. The results of motifs analysis showed that the number of motifs for samples with substrate temperatures of 600, 700, and 800°C is 1170, 689, and 158, respectively. This represents the growth of the crystalline structure of samples by raising the substrate temperature. Also the I–V graph showed that the resistivity of SiC films is ohmic and has an increasing trend with substrate temperature as expected from XRD and EDX results. According to the result of the statistical parameters, the kurtosis limit was more than 3 for sample a and less than 3 for samples b and c.

Acknowledgements

The authors would like to thank Mr. Soheil Pilehvar and Ms. Vahideh Mortazavi for their kind helps.

References

[1] Morelli D, Hermans J, Beetz C, Woo W S, Harris G L and Taylor C 1993 *Institut. Phys. Conf. Ser.* **137** 313

[2] Casady J B and Johnson R W 1996 *Solid State Electron.* **39** 1409

[3] Mehregany M, Zorman C A, Roy S, Fleischman A J, Wu C H and Rajan N 2000 *Inter. Mater. Rev.* **45** 85

[4] Yang Y T, Ekinci K L, Huang X M, Schiavone L M and Roukes M L 2001 *Appl. Phys. Lett.* **78** 162

[5] Liu W and Lieber C M 2006 *J. Phys. D: Appl. Phys.* **39** R387

[6] Thelander C and Agarwal P 2006 *Mater. Today* **9** 28

[7] Rao C N R, Deepak F L, Gundiah G and Govindaraj A 2003 *Progr. Solid State Chem.* **31** 5

[8] Wang Z L 2003 *Nanowires and nanobelts* (New York: Kluwer)

[9] Li Y, Qian F, Xiang J and Lieber C M 2006 *Mater. Today* **9** 18

[10] Zhang D H and Wang Y Y 2006 *Mater. Sci. Eng. B* **134** 9

[11] Samuelson L, Thelander C, Björk M T and Borgström M 2004 *Physica E* **25** 313

[12] http://www.lib.demokritos.gr/InTheNews/emerging0204.htm

[13] Ruff M, Mitlehner H and Helbig R 1994 *IEEE Trans. Electron. Devices* **41** 1040

[14] Morkoc H, Strite S, Gao G B, Lin M E, Sverdlov B and Burns M 1994 *J. Appl. Phys.* **76** 1363

[15] Cicero G, Catellani A and Galli G 2004 *Phys. Rev. Lett.* **93** 016102

[16] Dai H J, Wong E W, Lu Y Z, Fan S S and Lieber C M 1995 *Nature* **375** 769

[17] Mukherjee M 2011 ISBN: 978-953-307-968-4

[18] Andrievski R A 2009 *Rev. Adv. Mater. Sci.* **22** 1

[19] Snead L L, Nozawa T, Katoh Y, Byun T S, Kondo S and Petti D A 2007 *J. Nucl. Mater.* **371** 329

[20] Matsumoto S, Sato Y and Tusutumi M 1982 *J. Mater. Sci.* **17** 3106

[21] Woo H K, Lee C S, Bello I and Lee S T 1998 *J. Mater. Res.* **13** 1738

[22] Chen Y, Wang Z L, Yin J S, Johnson D J and Prince R H 1997 *Chem. Phys. Lett.* **272** 178

[23] Zhou X T, Wang N, Lai H L, Peng H Y, Bello I, Wong N B, Lee C S and Lee S T 1999 *Appl. Phys. Lett.* **74** 3942

[24] Chung G S and Kim K S 2007 *Bull. Korean Chem. Soc.* **28** 533

[25] Yoon S F, Ji R and Ahn J 1997 *Mater. Chem. Phys.* **49** 234

[26] Iliescu C and Poenar D P 2012 PECVD amorphous silicon carbide (α-SiC) layers for MEMS applications (InTech) Chap 5, ISBN 978-953-51-0917-4

[27] Fu Q G, Li H J, Shi X H, Wei J and Hu Z B 2006 *Mater. Chem. Phys.* **100** 108

[28] Al-Ruqeishi M S, Nor R M, Amin Y M and Al-Azri K 2010 *J. Alloys Compd.* **497** 272

[29] Chen K, Huang Z, Huang J, Fang M, Liu Y G, Ji H *et al* 2013 *Ceram. Inter.* **39** 1957

[30] Lin H, Gerbec J A, Sushkhid M and McFarland E W 2008 *Nanotechnology* **19** 325601

[31] Kopustinskas V, Meskinis S, Grigaliunas V, Tamulevicius S, Puceta M, Niaura G *et al* 2002 *Surf. Coat. Technol.* **151** 180

[32] Kopustinskas V, Meskinis S, Tamulevičius S, Andrulevičius M, Čižiūte B and Niaura G 2006 *Surf. Coat. Technol.* **200** 6240

[33] Roccaforte F, Giannazzo F, Iucolano F, Eriksson J, Weng M H and Raineri V 2010 *Appl. Surf. Sci.* **256** 5727

[34] Wu C H, Jacob C, Ning X J, Nishino S and Pirouz P 1996 *J. Cryst. Growth* **158** 480

[35] Johnson S G 1993 *Proc. SPIE* **2018** 237

[36] Daves W, Krauss A, Behnel N, Häublein V, Bauer A and Frey L 2011 *Thin Solid Films* **519** 5892

[37] Palmour J W 2006 *Mater. Sci. Forum* **527** 1129

[38] Battaile C C, Srolovitz D J, Oleinik I I, Pettifor D G, Sutton A P, Harris S J *et al* 1999 *J. Chem. Phys.* **111** 4291

[39] ISO 25178-2 2012 Geometrical product specifications (GPS) – surface texture: areal – part 2: Terms, definifions and surface texture parameters Available at: http://www.iso.org

[40] Alipour R, Meshkani S and Ghoranneviss M 2015 *Eur. Phys. J. Appl. Phys.* **71** 10302

[41] Mountains Map Premium (64-bit version) software Available at: http://www.digitalsurf.fr

[42] Johnson K L 1985 *Contact mechanics* (Cambridge University Press) p 407, ISBN 0-521-34796-3

[43] Stachowiak G W and Batchelor A W 2001 *Engineering tribology* (Boston: Butterworth-Heinemann) p 450, ISBN 0-7506-7304-4

[44] Douketis C, Wang Z, Haslett T L and Moskovits M 1995 *Phys. Rev. B* **51** 51